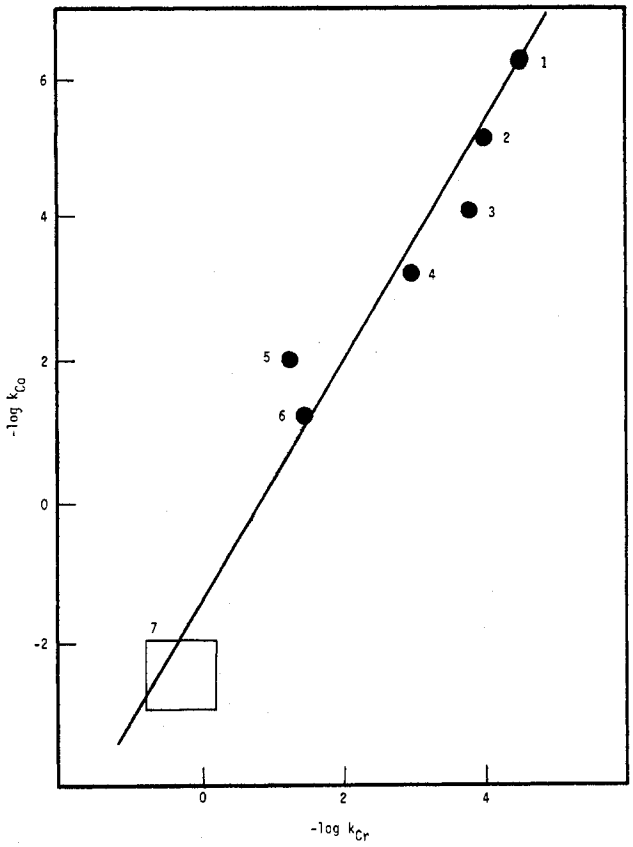

Figure 1. Linear free energy relationship of rate constants for aquation of Br^- from $M(L_4XBr^{n+})$ complexes. Points are (1) *trans*-$M(en)_2(NCS)Br^{n+}$, (2) $M(NH_3)_5Br^{2+}$, (3) *trans*-$M(en)_2Br_2^+$ corrected for statistical difference, (4) *cis*-$M(en)_2Br_2^+$ corrected for statistical difference, (5) *trans*-$M(en)_2(OH)Br^+$, (6) *cis*-$M(en)_2(OH)Br^+$, and (7) $M(NH_3)_4(NH_2)Br^+$ for the range of acidity constants of $M(NH_3)_5Br^{2+}$ of 10^{-15} to 10^{-16}.

complexes is considerably larger than those for Co(III) complexes, but by the point for *cis*-$M(en)_2OHBr^+$, the reverse order of rate constants prevails. The slope of the line drawn through these data is about 0.6, indicating this change in reactivity order.

We began this study anticipating that we would observe a change in slope in the curve in the figure. We reasoned that since $Cr(NH_3)_5Br^{2+}$ presumably substituted by an I_a pathway[1] and since the conjugate base path for this complex is presumably I_d,[1] then at some "directing" group intermediate in labilizing ability between NH_3 and NH_2^-, a mechanism change would occur. This change would cause a difference in slope. Clearly the data do not support the prediction.

There are three interpretations for the straight line behavior of the log–log plot and the value of the slope. If all of the Cr(III) and Co(III) aquations are assumed to be I_d and the activating pathway for these ligands is presumed to be their ability to π donate to relieve charge buildup in the dissociative transition state, then the lower demand for this donation in Cr(III), the least polarizing of the two cations, could account for the slope of less than 1. This view would presumably be endorsed by Ramasami and Sykes.[28] Alternatively, we could assume the mechanism for substitution at all the Cr(III) centers is associative interchange, whereas that at the Co(III) center is I_d. In this case the Cr(III) complexes have bond formation aiding in bond rupture and therefore have less requirement of charge supply by the "directing" groups. Thirdly, it is possible that both of the above mentioned phenomena are active, and the slopes generated by each coincide within the scatter caused by other properties of the complexes and the experimental error.

Registry No. *trans*-$Cr(en)_2OHBr^+$, 60933-53-1; *cis*-$Cr(en)_2OHBr^+$, 60886-01-3; *cis*-$[Cr(en)_2H_2OBr]Br_2$, 30172-32-8; *cis*-$[Cr(en)_2Cl_2]ClO_4$, 15654-71-4.

References and Notes

(1) T. W. Swaddle, *Coord. Chem. Rev.*, **14**, 217 (1974).
(2) T. W. Swaddle and G. Guastalla, *Inorg. Chem.*, **7**, 1915 (1968), and references therein.
(3) G. Guastalla and T. W. Swaddle, *Can. J. Chem.*, **51**, 821 (1973).
(4) C. H. Langford and H. B. Gray "Ligand Substitution Processes", W.A. Benjamin, New York, N.Y., 1965.
(5) C. H. Langford, *Inorg. Chem.*, **4**, 265 (1965).
(6) A. Haim, *Inorg. Chem.*, **9**, 426 (1970).
(7) Prepared by a modification of the procedure of M. Linhard and M. Weigel, *Z. Anorg. Allg. Chem.*, **271**, 115 (1952).
(8) W. W. Fee, C. S. Garner, and J. N. M. B. Harrowfield, *Inorg. Chem.*, **6**, 87 (1967).
(9) L. P. Quinn and C. S. Garner, *Inorg. Chem.*, **3**, 1348 (1964).
(10) W. W. Fee, J. N. M. B. Harrowfield, and W. G. Jackson, *J. Chem. Soc. A*, 2612 (1970).
(11) F. Woldbye, *Acta Chem. Scand.*, **12**, 1079 (1958).
(12) There is a slight drift in $[H^+]$ with time in these experiments because they are of low buffer capacity and the acidities of reactants and products differ. This drift does not affect our results in a substantial way.
(13) D. C. Olson and C. S. Garner, *Inorg. Chem.*, **2**, 558 (1963).
(14) F. R. Nordmeyer, *Inorg. Chem.*, **8**, 2780 (1969).
(15) D. A. Buckingham, P. A. Marzilli, and A. M. Sargeson, *Inorg. Chem.*, **8**, 1595 (1969).
(16) C. K. Poon, *Inorg. Chim. Acta Rev.*, **4**, 123 (1970).
(17) C. K. Ingold, R. S. Nyholm, and M. L. Tobe, *J. Chem. Soc.*, 1691 (1956).
(18) R. G. Linck, unpublished observations.
(19) A. W. Adamson and F. Basolo, *Acta Chem. Scand.*, **9**, 1261 (1955).
(20) M. A. Levine, T. P. Jones, W. E. Harris, and W. J. Wallace, *J. Am. Chem. Soc.*, **83**, 2453 (1961).
(21) T. W. Swaddle and W. E. Jones, *Can. J. Chem.*, **48**, 1054 (1970).
(22) S. C. Chan and M. L. Tobe, *J. Chem. Soc.*, 5700 (1963).
(23) A. M. Weiner and J. A. McLean, Jr., *Inorg. Chem.*, **3**, 1469 (1964).
(24) W. F. Cain and J. A. McLean, Jr., *Inorg. Chem.*, **4**, 1416 (1965).
(25) N. A. Maes, M. S. Nozari, and J. A. McLean, Jr., *Inorg. Chem.*, **12**, 750 (1973).
(26) S. C. Chan, K. Y. Hui, J. Miller, and W. S. Tsang, *J. Chem. Soc.*, 3207 (1965).
(27) D. A. Buckingham, I. I. Olsen, and A. M. Sargeson, *Inorg. Chem.*, **7**, 174 (1968).
(28) T. Ramasami and A. G. Sykes, *Inorg. Chem.*, **15**, 2885 (1976).

Contribution from the Department of Chemistry, State University of New York at Buffalo, Buffalo, New York 14214

An Accurate Redetermination of the Structure of Triruthenium Dodecacarbonyl, $Ru_3(CO)_{12}$

Melvyn Rowen Churchill,* Frederick J. Hollander, and John P. Hutchinson

Received February 23, 1977 AIC701353

We have recently determined the crystal structure of $H_2Os_3(CO)_{11}$ and have accurately redetermined (R_F = 3.35%; 3040 reflections) the structure of the isomorphous species $Os_3(CO)_{12}$.[1] These results show (inter alia) that the axial Os–CO bonds in $Os_3(CO)_{12}$ are lengthened relative to the equatorial Os–CO linkages (average values are 1.946 (6) and 1.912 (7) Å, respectively). This result is completely in accord with the accepted model for M–CO bonding and occurs as a result of competition for d_π electron density between the (mutually trans) axial carbonyl ligands.

The published crystal structure of $Ru_3(CO)_{12}$[2] is of relatively low precision (R_F = 7.9%; 936 reflections) and the reported Ru–CO bond lengths are such that the average Ru–CO (axial) distance of 1.89 (2) Å is slightly *shorter* than the average Ru–CO (equatorial) distance of 1.93 (2) Å.

As a result of this discrepancy, and with a firm belief that accurate molecular dimensions for all archetypal "binary"

Table I. Experimental Data for the X-ray Diffraction Study of $Ru_3(CO)_{12}$

(A) Crystal Parameters[a] at 23 °C

Crystal system: monoclinic	$\beta = 100.667\ (10)°$
Space group: $P2_1/n$[b]	$V = 1732.6\ (4)$ Å^3
$a = 8.1172\ (8)$ Å	$Z = 4$
$b = 14.8627\ (15)$ Å	ρ(calcd) = 2.450 g cm^{-3}
$c = 14.6140\ (20)$ Å	Mol wt 639.33

(B) Measurement of Intensity Data

Radiation: Mo Kα
Monochromator: highly oriented graphite (equatorial mode)
Reflections measd: $+h, +k, \pm l$
Scan type: θ(crystal) − 2θ(counter)
2θ range: 3–45°
Scan speed: 2.0°/min
Scan length: from $[2\theta(K\alpha_1) - 1.0]°$ to $[2\theta(K\alpha_2) + 1.0]°$
Background measurement: stationary crystal, stationary counter at beginning and end of each 2θ scan; each for half the time taken for the 2θ scan
Std reflections: three remeasured every 47 reflections; no significant changes in intensity were observed
Reflections collected: 2759 total, yielding 2281 independent reflections

[a] Unit cell parameters were derived from a least-squares fit to the setting angles of the unresolved Mo $K\bar{\alpha}$ components ($\bar{\lambda}$ 0.710 730 Å) of 24 reflections of the forms $\{6\bar{1}3\}$, $\{4\bar{6}4\}$, $\{3\bar{5}5\}$, $\{3\bar{1}8\}$, $\{0,10,1\}$, and $\{2\bar{9}4\}$, all with 2θ between 25 and 31°. [b] Equivalent positions are $\pm(x, y, z)$ and $\pm(^1/_2 + x, ^1/_2 - y, ^1/_2 + z)$. This represents a nonstandard setting of space group $P2_1/c$ [No. 14; C_{2h}^5].

Table II. Final Positional Parameters, with Esd's, for $Ru_3(CO)_{12}$[a]

Atom	x	y	z
Ru(1)	0.442 15 (4)	−0.023 22 (2)	0.223 02 (2)
Ru(2)	0.441 83 (4)	0.168 53 (2)	0.206 98 (2)
Ru(3)	0.694 33 (4)	0.080 59 (2)	0.338 23 (2)
C(11)	0.583 21 (53)	−0.029 86 (29)	0.129 04 (30)
O(11)	0.658 75 (42)	−0.041 82 (24)	0.071 98 (22)
C(12)	0.304 67 (52)	−0.013 54 (28)	0.317 06 (30)
O(12)	0.217 21 (42)	−0.016 30 (26)	0.369 91 (23)
C(13)	0.519 08 (56)	−0.139 23 (32)	0.270 11 (30)
O(13)	0.565 92 (47)	−0.207 11 (24)	0.298 48 (26)
C(14)	0.246 69 (58)	−0.049 44 (34)	0.129 97 (32)
O(14)	0.131 96 (44)	−0.065 77 (29)	0.076 51 (26)
C(21)	0.588 24 (55)	0.160 38 (28)	0.115 25 (31)
O(21)	0.666 56 (45)	0.163 80 (24)	0.058 94 (24)
C(22)	0.297 80 (56)	0.175 06 (32)	0.298 29 (33)
O(22)	0.208 47 (46)	0.187 08 (30)	0.348 08 (26)
C(23)	0.249 39 (57)	0.182 10 (32)	0.107 93 (32)
O(23)	0.137 38 (45)	0.191 61 (29)	0.051 16 (25)
C(24)	0.517 87 (57)	0.288 27 (33)	0.237 40 (32)
O(24)	0.563 82 (47)	0.358 22 (25)	0.258 12 (28)
C(31)	0.835 83 (52)	0.071 46 (26)	0.244 36 (30)
O(31)	0.930 83 (39)	0.067 65 (21)	0.197 05 (23)
C(32)	0.550 04 (52)	0.095 50 (28)	0.429 46 (30)
O(32)	0.482 05 (40)	0.106 45 (22)	0.489 39 (22)
C(33)	0.821 36 (53)	0.182 12 (32)	0.391 01 (30)
O(33)	0.895 29 (44)	0.242 66 (24)	0.423 24 (26)
C(34)	0.809 59 (52)	−0.019 68 (30)	0.405 61 (28)
O(34)	0.876 25 (43)	−0.078 32 (22)	0.444 80 (24)

[a] Esd's shown in parentheses are right-adjusted to the last digit of the preceding number.

metal carbonyls should be available, we have undertaken a redetermination of the crystal structure of $Ru_3(CO)_{12}$. Our results are reported below.

Experimental Section

A crystal of approximate dimensions 0.3 mm × 0.15 mm × 0.15 mm was selected from a sample purchased from Ventron Corp. The crystal was mounted with its extended c^* direction close to the goniometer ϕ axis; the quality of the diffraction pattern was checked photographically and found to be satisfactory. The crystal was then transferred to a Syntex $P2_1$ diffractometer. Crystal alignment, determination of cell parameters, and data collection were carried out as described previously.[3] Details appear in Table I.

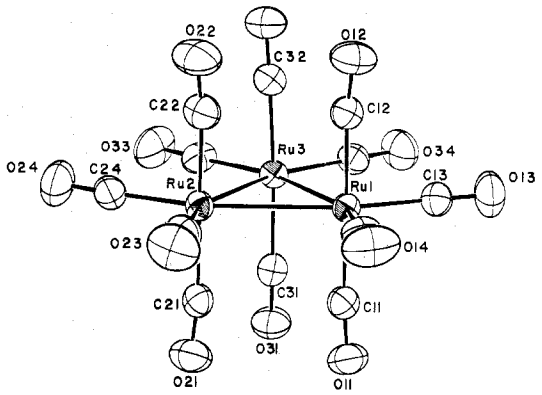

Figure 1. $Ru_3(CO)_{12}$, viewed from a direction 75° from the normal to the Ru_3 plane [ORTEP2 diagram; 50% ellipsoids].

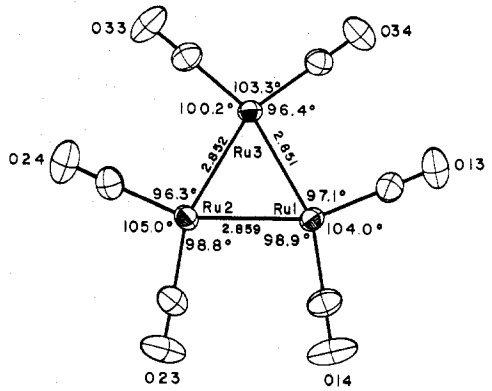

Figure 2. Distribution of equatorial ligands in the Ru_3 plane of the $Ru_3(CO)_{12}$ molecule [ORTEP2; 50% ellipsoids].

All crystallographic computations were performed using the Syntex XTL system[4] [NOVA 1200 computer with 24K, 16-bit word memory; disk unit of 1.2 million words; XTL conversational program package, as modified at SUNYAB].

Data were corrected for absorption by an empirical method. Seven close-to-axial reflections, distributed over the range of 2θ values used in data collection, each of fairly strong intensity, were measured at 36 points around the diffraction vector (from $\psi = 0°$ to $\psi = 350°$, $\Delta\psi = 10°$). Each reflection was used to define a normalized absorption curve vs. ϕ, corrected for ω and χ. The curves bracketing the 2θ value of the reflection under consideration were interpolated both in 2θ and in ϕ to derive the absorption correction for the intensity of that reflection. Reflections used for the absorption curves[5] were $00\bar{4}$ [2θ = 11.34°, (minimum intensity)/(maximum intensity) = 0.762], $01\bar{5}$ [14.45°, 0.773], $00\bar{8}$ [22.79°, 0.739], $10\bar{9}$ [25.23°, 0.725], $0,1,\bar{1}\bar{1}$ [31.65, 0.762], $1,0,\bar{1}\bar{3}$ [36.82°, 0.769], and $0,0,\bar{1}\bar{4}$ [40.45°, 0.757]. All curves were mutually consistent—i.e., maximum and minimum corrections were observed at essentially the same values of ϕ and all curves had similar profiles.

Redundant and equivalent data were averaged [$R_{av} = (\sum|I - I_{av}|/\sum I) = 0.019$ for 188 averaged pairs of data] and were converted to unscaled $|F_o|$ values after correction for Lorentz and polarization effects. A value of $|F_o| = 0.0$ was assigned to any reflection with measured $I < 0$. The esd's, $\sigma_c(|F_o|)$, were based on the larger of (i) counting statistics or (ii) the internal esd obtained by averaging symmetry-equivalent reflections.

The structural analysis was begun using the positional and isotropic thermal parameters from our study on $Os_3(CO)_{12}$.[1,6,7] Full-matrix least-squares refinement of all positional and isotropic thermal parameters converged after 4 cycles with $R_F = 5.3\%$, $R_{wF} = 6.5\%$, and GOF = 2.39.[8] Continued refinement, using anisotropic thermal parameters for all atoms, converged in 3 cycles with $R_F = 3.4\%$, $R_{wF} = 3.9\%$, and GOF = 1.41. At this stage it became apparent that secondary extinction was affecting the very strong low-order reflections. $|F_o|$ values were corrected using the approximate eq 1, derived from

$$|F_o|_{cor} = |F_o|_{uncor}(1.0 + gI_o) \quad (1)$$

Table III. Final Anisotropic Thermal Parameters,[a] with Esd's, for $Ru_3(CO)_{12}$

Atom	B_{11}	B_{22}	B_{33}	B_{12}	B_{13}	B_{23}
Ru(1)	2.29 (2)	2.34 (2)	2.38 (2)	−0.28 (1)	0.27 (1)	−0.17 (1)
Ru(2)	2.38 (2)	2.38 (2)	2.76 (2)	0.32 (1)	0.35 (1)	0.35 (1)
Ru(3)	1.97 (2)	2.45 (2)	2.18 (2)	−0.09 (1)	0.13 (1)	−0.02 (1)
C(11)	3.20 (20)	3.06 (20)	3.05 (19)	−0.45 (16)	0.30 (17)	−0.21 (16)
O(11)	5.02 (17)	4.83 (17)	3.88 (16)	−0.40 (14)	1.90 (14)	−0.85 (14)
C(12)	2.90 (20)	3.15 (20)	3.13 (20)	−0.42 (15)	0.34 (17)	−0.19 (15)
O(12)	4.10 (17)	6.59 (22)	3.96 (16)	−1.05 (14)	1.44 (14)	−0.46 (14)
C(13)	3.63 (20)	3.01 (23)	3.50 (20)	−0.32 (17)	0.69 (16)	−0.09 (17)
O(13)	6.67 (22)	3.02 (17)	6.66 (21)	0.48 (15)	1.34 (16)	0.87 (15)
C(14)	2.92 (21)	4.81 (24)	3.29 (20)	−0.49 (18)	0.75 (17)	−0.76 (18)
O(14)	3.69 (18)	10.01 (29)	4.61 (18)	−1.34 (17)	−0.24 (15)	−2.16 (18)
C(21)	3.38 (21)	2.88 (20)	3.18 (20)	0.67 (15)	0.23 (18)	0.45 (16)
O(21)	5.11 (18)	5.71 (20)	3.88 (16)	1.38 (14)	1.65 (15)	1.10 (14)
C(22)	3.23 (22)	4.21 (23)	3.86 (21)	0.95 (17)	0.62 (18)	0.83 (18)
O(22)	4.69 (19)	7.59 (24)	5.73 (19)	2.15 (16)	2.53 (17)	1.49 (17)
C(23)	3.27 (22)	3.93 (22)	3.69 (21)	0.46 (17)	0.53 (19)	0.74 (18)
O(23)	3.96 (17)	8.55 (25)	4.96 (18)	0.76 (17)	−1.00 (15)	1.23 (18)
C(24)	3.86 (22)	3.16 (23)	4.05 (22)	0.18 (18)	1.27 (17)	0.46 (18)
O(24)	6.93 (23)	3.31 (18)	7.56 (23)	−0.70 (16)	2.20 (18)	−1.03 (17)
C(31)	2.40 (18)	2.71 (19)	2.88 (19)	−0.03 (14)	−0.09 (16)	−0.12 (14)
O(31)	3.18 (15)	4.81 (18)	3.94 (15)	0.20 (12)	1.26 (13)	0.02 (12)
C(32)	2.74 (19)	3.24 (20)	2.94 (20)	−0.25 (15)	0.34 (16)	0.09 (15)
O(32)	4.24 (16)	5.23 (18)	3.56 (15)	0.21 (14)	1.48 (13)	−0.01 (14)
C(33)	2.93 (20)	3.65 (22)	3.33 (19)	−0.27 (17)	0.73 (15)	−0.60 (17)
O(33)	4.73 (17)	4.79 (18)	6.34 (19)	−1.99 (15)	1.18 (15)	−2.26 (16)
C(34)	2.88 (19)	3.23 (21)	2.86 (19)	−0.05 (16)	0.47 (15)	0.17 (17)
O(34)	4.66 (17)	4.51 (17)	4.62 (18)	1.21 (14)	0.42 (14)	1.39 (14)

[a] These anisotropic thermal parameters are analogous to the usual form of the isotropic thermal parameter and have units of Å^2. They enter the expression for the structure factor in the form $\exp[-0.25(B_{11}h^2a^{*2} + B_{22}k^2b^{*2} + B_{33}l^2c^{*2} + 2B_{12}hka^*b^* + 2B_{13}hla^*c^* + 2B_{23}klb^*c^*)]$.

Zachariasen's treatment.[9] The value of g (2.0×10^{-7}) was determined graphically. Continued refinement led to final convergence [$(\Delta/\sigma)_{max} = 0.05$ for a positional and 0.09 for a thermal parameter] in 2 cycles with $R_F = 2.6\%$, $R_{wF} = 2.8\%$, and GOF = 1.04. The correctness of the structure was confirmed by means of a final difference-Fourier synthesis on which the highest peak was of height 0.48 e Å^{-3}.

Throughout the analysis, the analytical scattering factors of Cromer and Mann for *neutral* atoms were used;[10a] both the real and imaginary components of anomalous dispersion were included for all atoms.[10b] The weighting scheme used was that of eq 2, with $p = 0.02$. All 2281

$$w = [(\sigma_c(|F_o|))^2 + (p|F_o|)^2]^{-1} \quad (2)$$

unique data were included in the refinement.

Final positional and anisotropic thermal parameters are collected in Tables II and III.

Discussion

Figure 1 shows a general view of the $Ru_3(CO)_{12}$ molecule. Interatomic distances and angles are listed in Tables IV and V. Deviations of atoms from the Ru_3 plane are given in Table VI; the distribution of equatorial ligands in this plane is illustrated in Figure 2.

Estimated standard deviations in our present study are approximately one-tenth to one-fifteenth of those reported in the determination of Mason and Rae.[2] The increased precision allows the following conclusions to be reached.

(1) In agreement with our previous study on $Os_3(CO)_{12}$[1] and in contradistinction to the Mason/Rae study of $Ru_3(CO)_{12}$,[2] the axial Ru–CO bond lengths are, indeed, longer than the equatorial Ru–CO linkages. Axial Ru–CO bonds range in length from 1.929 (4) to 1.953 (5) Å, averaging 1.942 [4] Å; equatorial Ru–CO distances range from 1.908 (5) to 1.934 (5) Å, averaging 1.921 [5] Å. The significance of this result is confirmed by the observation that the axial Ru···O vectors are also longer [range 3.060 (4)–3.078 (4) Å; average 3.071 [3] Å] than the equatorial Ru···O vectors [range 3.035 (4)–3.055 (3) Å; average 3.048 [3] Å], notwithstanding the fact that the axial Ru–C–O systems are *bent* whereas the equatorial Ru–C–O systems are *linear* (see (2)).

Table IV. Interatomic Distances (Å) with Esd's for $Ru_3(CO)_{12}$

(A) Ruthenium–Ruthenium			
Ru(1)–Ru(2)	2.8595 (4)	Ru(2)–Ru(3)	2.8518 (4)
Ru(1)–Ru(3)	2.8512 (4)		
(B) Ru–C and Ru···O (Axial)			
Ru(1)–C(11)	1.947 (4)	Ru(1)···O(11)	3.078 (3)
Ru(1)–C(12)	1.929 (4)	Ru(1)···O(12)	3.067 (3)
Ru(2)–C(21)	1.953 (5)	Ru(2)···O(21)	3.078 (4)
Ru(2)–C(22)	1.932 (5)	Ru(2)···O(22)	3.060 (4)
Ru(3)–C(31)	1.950 (4)	Ru(3)···O(31)	3.073 (3)
Ru(3)–C(32)	1.943 (4)	Ru(3)···O(32)	3.067 (3)
	Av 1.942 [4][a]		Av 3.071 [3][a]
(C) Ru–C and Ru···O (Equatorial)			
Ru(1)–C(13)	1.918 (5)	Ru(1)···O(13)	3.047 (4)
Ru(1)–C(14)	1.929 (5)	Ru(1)···O(14)	3.054 (4)
Ru(2)–C(23)	1.934 (5)	Ru(2)···O(23)	3.054 (4)
Ru(2)–C(24)	1.909 (5)	Ru(2)···O(24)	3.035 (4)
Ru(3)–C(33)	1.908 (5)	Ru(3)···O(33)	3.042 (4)
Ru(3)–C(34)	1.930 (4)	Ru(3)···O(34)	3.055 (3)
	Av 1.921 [5][a]		Av 3.048 [3][a]
(D) C–O (Axial)			
C(11)–O(11)	1.137 (5)	C(31)–O(31)	1.128 (5)
C(12)–O(12)	1.142 (5)	C(32)–O(32)	1.130 (5)
C(21)–O(21)	1.130 (6)		Av 1.133 [2][a]
C(22)–O(22)	1.133 (6)		
(E) C–O (Equatorial)			
C(13)–O(13)	1.130 (6)	C(33)–O(33)	1.134 (6)
C(14)–O(14)	1.126 (6)	C(34)–O(34)	1.125 (5)
C(23)–O(23)	1.121 (6)		Av 1.127 [2][a]
C(24)–O(24)	1.127 (6)		
(F) C···C and O···O (Axial, Nonbonding)			
C(11)···C(21)	2.835 (6)	O(11)···O(21)	3.063 (5)
C(11)···C(31)	2.834 (6)	O(11)···O(31)	3.061 (5)
C(21)···C(31)	2.818 (6)	O(21)···O(31)	3.019 (5)
C(12)···C(22)	2.816 (6)	O(12)···O(22)	3.039 (6)
C(12)···C(32)	2.843 (6)	O(12)···O(32)	3.100 (5)
C(22)···C(32)	2.795 (6)	O(22)···O(32)	2.989 (5)

[a] Error estimates shown in brackets for average distances, $\bar{d}$, are the exterior estimates of the precision of the average value given by $[\Sigma_n(\bar{d} - d)^2/(n^2 - n)]^{1/2}$.

Table V. Interatomic Angles (deg) with Esd's for $Ru_3(CO)_{12}$

	(A) Within the Ru_3 Triangle		
Ru(2)-Ru(1)-Ru(3)	59.92 (1)	Ru(2)-Ru(3)-Ru(1)	60.18 (1)
Ru(1)-Ru(2)-Ru(3)	59.90 (1)		
	(B) Ru-Ru-CO (Equatorial)		
Ru(2)-Ru(1)-C(14)	98.94 (14)	Ru(3)-Ru(2)-C(24)	96.28 (14)
Ru(1)-Ru(2)-C(23)	98.84 (14)	Ru(1)-Ru(3)-C(34)	96.35 (13)
Ru(3)-Ru(1)-C(13)	97.13 (13)	Ru(2)-Ru(3)-C(33)	100.18 (13)
	(C) OC-Ru-CO (Equatorial-Equatorial)		
C(13)-Ru(1)-C(14)	104.01 (20)	C(33)-Ru(3)-C(34)	103.28 (18)
C(23)-Ru(2)-C(24)	104.99 (20)		
	(D) Ru-Ru-CO (Axial)		
Ru(2)-Ru(1)-C(11)	89.11 (13)	Ru(1)-Ru(2)-C(22)	89.14 (14)
Ru(3)-Ru(1)-C(11)	89.56 (13)	Ru(3)-Ru(2)-C(22)	90.57 (14)
Ru(2)-Ru(1)-C(12)	89.56 (13)	Ru(1)-Ru(3)-C(31)	89.94 (12)
Ru(3)-Ru(1)-C(12)	89.18 (13)	Ru(2)-Ru(3)-C(31)	90.13 (12)
Ru(1)-Ru(2)-C(21)	90.17 (13)	Ru(1)-Ru(3)-C(32)	90.51 (13)
Ru(3)-Ru(2)-C(21)	88.88 (13)	Ru(2)-Ru(3)-C(32)	87.70 (13)
	(E) OC-Ru-CO (Axial-Equatorial)		
C(11)-Ru(1)-C(13)	90.73 (19)	C(22)-Ru(2)-C(23)	90.20 (20)
C(11)-Ru(1)-C(14)	90.39 (19)	C(22)-Ru(2)-C(24)	90.18 (20)
C(12)-Ru(1)-C(13)	90.24 (19)	C(31)-Ru(3)-C(33)	89.70 (18)
C(12)-Ru(1)-C(14)	90.49 (19)	C(31)-Ru(3)-C(34)	90.69 (18)
C(21)-Ru(2)-C(23)	90.15 (19)	C(32)-Ru(3)-C(33)	88.96 (18)
C(21)-Ru(2)-C(24)	90.35 (19)	C(32)-Ru(3)-C(34)	92.00 (18)
	(F) OC-Ru-CO (Axial-Axial)		
C(11)-Ru(1)-C(12)	178.50 (18)	C(31)-Ru(3)-C(32)	177.21 (18)
C(21)-Ru(2)-C(22)	179.27 (19)		
	(G) Ru-C-O (Axial)		
Ru(1)-C(11)-O(11)	173.26 (39)	Ru(2)-C(22)-O(22)	173.10 (42)
Ru(1)-C(12)-O(12)	173.03 (38)	Ru(3)-C(31)-O(31)	173.14 (37)
Ru(2)-C(21)-O(21)	173.07 (39)	Ru(3)-C(32)-O(32)	172.28 (38)
	(H) Ru-C-O (Equatorial)		
Ru(1)-C(13)-O(13)	179.22 (41)	Ru(2)-C(24)-O(24)	177.91 (43)
Ru(1)-C(14)-O(14)	178.93 (43)	Ru(3)-C(33)-O(33)	179.01 (40)
Ru(2)-C(23)-O(23)	178.64 (43)	Ru(3)-C(34)-O(34)	179.75 (39)

Table VI. Deviations of Atoms (Å) from the Ru_3 Plane

Equation of Plane:[a] $0.7188X - 0.0662Y - 0.6921Z + 0.0476 = 0$

C(11)	1.946 (4)	C(13)	0.003 (5)
O(11)	3.077 (3)	O(13)	0.006 (4)
C(12)	−1.929 (4)	C(14)	−0.009 (5)
O(12)	−3.065 (3)	O(14)	−0.027 (4)
C(21)	1.952 (5)	C(23)	0.041 (5)
O(21)	3.075 (4)	O(23)	0.053 (4)
C(22)	−1.932 (5)	C(24)	−0.036 (5)
O(22)	−3.057 (4)	O(24)	−0.083 (4)
C(31)	1.950 (4)	C(33)	0.014 (4)
O(31)	3.070 (3)	O(33)	0.003 (4)
C(32)	−1.941 (4)	C(34)	−0.029 (4)
O(32)	−3.060 (3)	O(34)	−0.049 (4)

[a] Orthonormal (Å) coordinates (X, Y, Z) are related to the fractional coordinates (x, y, z) by the transformation: $X = ax + cz \cdot \sin\beta$, $Y = by$, $Z = cz \sin\beta$.

(2) The equatorial Ru–C–O moieties are all very close to linear, individual values of the Ru–C–O angle varying from 177.91 (43)° to 179.75 (39)°. In contrast to this, each axial Ru–C–O moiety is distorted from linearity by about 7°. Individual Ru–C–O angles range from 172.28 (38) to 173.26 (39)°. The cause of this distortion is straightforward—it is the result of van der Waals repulsions between axial oxygen atoms. Thus, ruthenium–ruthenium distances range from 2.8512 (4) to 2.8595 (4) Å; C(axial)···C(axial) contacts range from 2.795 (6) to 2.843 (6) Å [i.e., similar to the mean Ru–Ru distance], but O(axial)···O(axial) contacts are expanded to 2.989 (5)–3.100 (5) Å.

(3) The ruthenium–ruthenium bonds within the Ru_3 triangle are not strictly equivalent. The Ru(1)–Ru(2) bond length of 2.8595 (4) Å is slightly longer than the Ru(1)–Ru(3) and Ru(2)–Ru(3) bonds [2.8512 (4) and 2.8518 (4) Å; average 2.8515 [4] Å]. The difference of 0.0080 ± 0.0006 Å is slight and probably of little energetic significance. However, it is duplicated in $Os_3(CO)_{12}$[1] [Os(1)–Os(2) = 2.8824 (5) Å vs. Os(1)–Os(3) = 2.8752 (5) Å and Os(2)–Os(3) = 2.8737 (5) Å; difference 0.0079 ± 0.0011 Å] and presumably results from crystal forces.

(4) Within the equatorial plane, Ru–Ru–CO angles vary from 96.28 (14) to 100.18 (13)° [average 97.95°] while OC–Ru–CO angles range from 103.28 (18) to 104.99 (20)° [average 104.09°].

(5) The equatorial carbonyl ligands lie very close to the Ru_3 plane, the maximum deviation of a carbon atom being 0.041 (5) Å and the maximum deviation of an oxygen atom being 0.083 (4) Å.

(6) Based on average Ru–Ru and Os–Os bond lengths in $Ru_3(CO)_{12}$ and $Os_3(CO)_{12}$,[1] covalent radii of the zerovalent metal ions are 1.427 Å for Ru(0) and 1.439 Å for Os(0). The closeness of these two values results from the lanthanide contraction.

Acknowledgment. This work was generously supported by the National Science Foundation through Grants No. CHE76-05564 and CHE77-04981, to M. R. Churchill.

Registry No. $Ru_3(CO)_{12}$, 15243-33-1.

Supplementary Material Available: Lising of structure factor amplitudes (10 pages). Ordering information is given on any current masthead page.

References and Notes

(1) M. R. Churchill and B. G. DeBoer, *Inorg. Chem.*, **16**, 878 (1977).
(2) R. Mason and A. I. M. Rae, *J. Chem. Soc. A*, 778 (1968).
(3) M. R. Churchill, R. A. Lashewycz, and F. J. Rotella, *Inorg. Chem.*, **16**, 265 (1977).
(4) "Syntex XTL Operations Manual", 2nd ed, Syntex Analytical Instruments, Cupertino, Calif., 1976.

(5) The calculated absorption coefficient for Mo Kα radiation is $\mu = 25.8$ cm^{-1}.
(6) The original structural study of $Os_3(CO)_{12}$,[7] was based on space group $P2_1/n$ as was our redetermination of this structure.[1] The determination of $Ru_3(CO)_{12}$ by Mason and Rae[2] was based upon space group $P2_1/c$; our redetermination of this structure is based instead upon space group $P2_1/n$ so all results will be directly comparable with those obtained on $Os_3(CO)_{12}$. The structures of $Os_3(CO)_{12}$ and $Ru_3(CO)_{12}$ are isomorphous.
(7) E. R. Corey and L. F. Dahl, *Inorg. Chem.*, **1**, 521 (1962).
(8) $R_F = 100\sum||F_o| - |F_c||/\sum|F_o|$; $R_{wF} = 100[\sum w(|F_o| - |F_c|)^2/\sum w|F_o|^2]^{1/2}$; GOF = $[\sum w(|F_o| - |F_c|)^2/(n-m)]^{1/2}$, where n is the number of reflections and m is the number of variables.
(9) W. H. Zachariasen, *Acta Crystallogr.*, **16**, 1139 (1963); see also G. H. Stout and L. H. Jensen, "X-Ray Structure Determination", Macmillan, London, 1968, pp 411–412, especially eq 17.16.
(10) "International Tables for X-Ray Crystallography", Vol. 4, Kynoch Press, Birmingham, England, 1974: (a) Table 2.2B, pp 99–101; (b) Table 2.3.1, pp 149–150.

Contribution from the Department of Chemistry, University of California, and the Materials and Molecular Research Division, Lawrence Berkeley Laboratory, Berkeley, California 94720, the Department of Chemistry, University of Western Ontario, London, Ontario N6A 3K7, Canada, and the Institute of Physics, S-751 21 Uppsala, Sweden

ESCA Spectra of Trimethylenemethaneiron Tricarbonyl and Butadieneiron Tricarbonyl

J. W. Koepke,[1a] W. L. Jolly,*[1a] G. M. Bancroft,[1b] P. Å. Malmquist,[1c] and K. Siegbahn[1c]

Received February 9, 1977 AIC70107K

The trimethylenemethane diradical (I) has been the subject

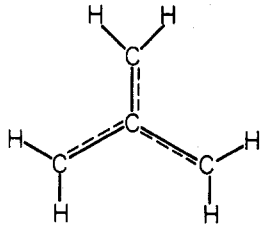

I

of considerable theoretical speculation.[2,3] It has been detected only at low concentrations as an unstable intermediate.[3a] An ab initio calculation by Yarkony and Schaefer[4] indicated that the central carbon has a charge of +0.62, comparable to the charge of the carbon atom in CHF_3. Although trimethylenemethane itself is too unstable to allow investigation of its charge distribution by ESCA, we have studied the ESCA spectrum of the relatively stable complex trimethylenemethaneiron tricarbonyl.[5] For comparison we have also studied the structural isomer butadieneiron tricarbonyl.

Savariaut and Labarre[6] reported, on the basis of CNDO/2 calculations, that the bonds between the iron atom and the three CH_2 groups of trimethylenemethaneiron tricarbonyl are much stronger than the bond between the iron atom and the central carbon. They calculated atomic charges of +0.67 for the iron atom, +0.09 for the carbonyl carbon atoms, −0.30 for the CH_2 carbon atoms, and +0.17 for the central carbon atom and explained the weak bond between the iron atom and the central carbon atom in terms of electrostatic repulsion. We hoped that measurement of the carbon 1s binding energies of the compound would give enough information regarding the charge distribution in the molecule to test these calculations.

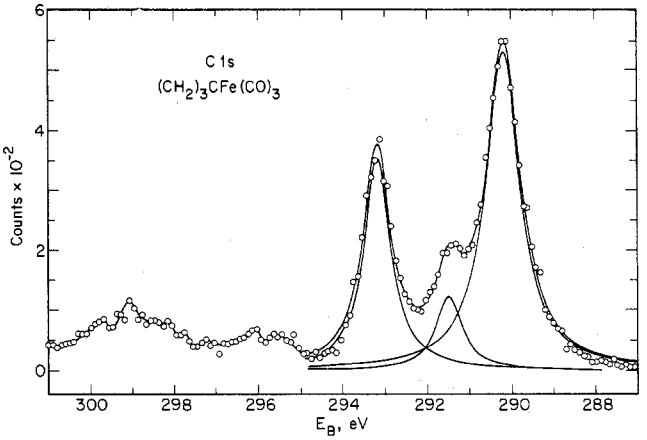

Figure 1. Carbon 1s spectrum of trimethylenemethaneiron tricarbonyl, deconvoluted using Lorentzian curves. The relative intensities of the three peaks are 2.96:1:5.72.

Trimethylenemethane has been implicated as an intermediate in several reactions,[7] and our results will determine whether ESCA can serve as a tool to search for trimethylenemethane intermediates on catalyst surfaces.

Experimental Section

Butadieneiron tricarbonyl was prepared as described by King[8] and was identified by its infrared spectrum[9] and NMR spectrum. Trimethylenemethaneiron tricarbonyl was prepared by the reaction of 3-chloro-2-methylpropene with $Fe_2(CO)_9$.[5] Both the IR and NMR spectra were consistent with the literature.[5]

Both ESCA spectra were obtained in the gas phase. The spectrum of trimethylenemethaneiron tricarbonyl was recorded on the Uppsala electrostatic high-resolution spectrometer.[10] The C 1s and O 1s lines of carbon monoxide were used as references. We used 296.22 and 542.57 eV for the C 1s and O 1s binding energies of CO, respectively; these are averages of the values obtained by Smith and Thomas[11] and Perry and Jolly.[12] The Fe $2p_{3/2}$ binding energy of trimethylenemethaneiron tricarbonyl was measured relative to the F 1s binding energy of CF_4, using 695.55 eV for the latter binding energy (an average of literature values[13,14]). The reference gases and sample vapors were run simultaneously. The spectrum of butadieneiron tricarbonyl was recorded on the old Berkeley magnetic spectrometer.[15] Argon was introduced with the sample, and the Ar $2p_{3/2}$ line (E_B = 248.62 eV)[16] was used as a reference for all lines of butadieneiron tricarbonyl. Sample and reference lines were scanned alternately. The best least-squares fitting of the data was obtained assuming Lorentzian curves in the case of trimethylenemethaneiron tricarbonyl and Gaussian curves in the case of butadieneiron tricarbonyl.

Results and Discussion

The C 1s spectra are shown in Figures 1 and 2, and Table I lists all the binding energies. The smaller line widths obtained for trimethylenemethaneiron tricarbonyl reflect the better resolution of the Uppsala instrument. The peaks are easily assigned by comparison with the binding energies of other organometallic compounds and by intensity considerations. The peaks at 293.17 eV in Figure 1 and at 293.03 eV in Figure 2 are in the region typical of metal carbonyls and can be confidently assigned to the CO groups in the compounds. In Figure 1, the relatively weak peak at 291.47 eV is undoubtedly due to the central carbon, and the 290.18-eV peak is due to the CH_2 groups. The CO peaks in both spectra and the central carbon peak in Figure 1 have lost considerable intensity to shake up bands at higher energy. In the case of butadieneiron tricarbonyl our results can be compared with those of Connor et al.,[17] who obtained an ESCA spectrum of this compound in the gas phase. Their reported C 1s and O 1s binding energies are 0.3–0.4 eV higher than ours, whereas their Fe $2p_{3/2}$ value is essentially the same as ours. The discrepancies are not unreasonable in view of their estimated accuracy of ±0.2 eV. The intensity ratio of the C 1s peaks due to the CO